Fang-Chi Li, DDS, PhD,[*] Eric Nicholson, BEng,[†] Chandra Veer Singh, BEng, PhD,[†] and Anil Kishen, BDS, MDS, PhD[*]

Microtissue Engineering Root Dentin with Photodynamically Cross-linked Nanoparticles Improves Fatigue Resistance of Endodontically Treated Teeth

SIGNIFICANCE

This study highlighted the potential of microtissue engineering root canal dentin with photodynamically cross-linked nanoparticles to improve radicular strain distribution and resistance to fatigue loads in endodontically treated teeth.

ABSTRACT

Introduction: Microtissue engineering root canal dentin with biopolymeric nanoparticles has the potential to improve mechanical properties of iatrogenically compromised root dentin. This study aims to characterize the surface mechanical property, bulk biomechanical response, and fatigue resistance of microtissue-engineered root dentin using photodynamically (photodynamic-activated [PDA]) cross-linked chitosan nanoparticles (CSnps). **Methods:** Experiments were conducted in 3 parts: part 1, root canal dentin sections were subjected to nanoindentations before/after treatment with CSnps and chemically (1-ethyl-3-[3-dimethylaminopropyl]carbodiimide [EDC] cross-linked CSnps) and photodynamically cross-linked CSnps to determine the properties of treated surfaces ($n = 84$ points/group); part 2, root canal dentin specimens treated with PDA cross-linked CSnps were subjected to strain analysis using customized moiré interferometry ($n = 5$/group); and part 3, root canal dentin specimens treated with EDC cross-linked CSnps, PDA cross-linked CSnps, and instrumented controls were tested using an accelerated fatigue loading protocol to evaluate the sustained loads and cycles at failure ($n = 15$/group). Data were analyzed using the paired sample *t* test, trend analysis, and Kaplan-Meier with log-rank tests at a significance of .05 in each experiment. **Results:** Root dentin microtissue engineered with PDA cross-linked CSnps showed a 16.8% increase in elastic modulus and a conspicuous decrease in strain distribution in cervical root dentin ($P < .01$). There was a significant reduction in the tensile strain formed at the apical region of the instrumented root dentin after treatment ($P < .05$). Survival analysis showed a statistically significant difference ($P < .05$) among evaluated conditions in fatigue resistance (ie, PDA cross-linked CSnps > EDC cross-linked CSnps > control). **Conclusions:** This study highlighted the potential of root canal dentin microtissue engineering with PDA cross-linked CSnps to diminish radicular strain distribution and improve resistance to fatigue loads in endodontically treated teeth. *(J Endod 2020;46:668–674.)*

KEY WORDS

Endodontically treated teeth; fatigue resistance; microtissue-engineered dentin; nanoparticles; photodynamic cross-link

From the *Faculty of Dentistry, and [†]Department of Materials Science and Engineering, University of Toronto, Toronto, Ontario, Canada

Address requests for reprints to Dr Anil Kishen, Faculty of Dentistry, University of Toronto, 124 Edward Street, Toronto, Ontario, Canada M5G 1G6.
E-mail address: anil.kishen@dentistry.utoronto.ca
0099-2399/$ - see front matter

https://doi.org/10.1016/j.joen.2020.01.021

Vertical root fracture (VRF) is the third reason of failure in endodontically extracted teeth representing 6%–13.4%, which frustrates both clinicians and patients[1,2]. Many physiological, pathologic, and iatrogenic factors have been attributed to the compromised mechanical integrity of restored root-filled teeth[3,4]. The increased loss of tooth structure in endodontically treated teeth also alters the radicular stress distribution pattern, resulting in higher stress distribution in the apical region and root flexure, particularly along the buccal-lingual plane of the root. This altered biomechanical response can contribute to the higher prevalence of VRF in nonvital teeth[5]. To date, there is no available treatment methods that can counteract

the adverse effects of disease/treatment-mediated changes in the root dentin structure of endodontically treated teeth.

The process of microtissue engineering aims to design tissues of improved biological and mechanical characteristics to support tissue function, cell behavior, and host integration[6]. One strategy to improve mechanical properties of dentin tissue involves 2 steps. The first step is to induce more numbers of molecular collagen cross-links with synthetic/natural chemicals[7]. The second step is to infiltrate biopolymeric nanofillers into dentin matrix[8]. At a microscale, the microtissue-engineered dentin matrix would present a stabilized dentin surface ultrastructure with enhanced mechanical characteristics, bioactivity, and resistance to host/bacteria-mediated enzymatic degradation[8–10]. Chemical cross-linking is commonly used to stabilize the collagen-based materials. However, consideration needs to be taken regarding some drawbacks such as prolonged treatment time, cytotoxicity, and possible pigmentation[11]. As an alternative to chemical cross-linking, photodynamic-activated (PDA) cross-linking has been reported to induce rapid and stable covalent cross-linking of collagen. This is attained by exposing a photosensitizer to an appropriate wavelength of light[12,13]. Thus, rose Bengal [RB]–functionalized chitosan nanoparticles (CSRBnps), which incorporated a photosensitizer (rose bengal) in CSnps, has dual advantages of generating PDA cross-linking and providing biopolymeric nanofillers for effective microtissue engineering of root canal dentin[14]. The aim of the current study was to evaluate the surface properties, biomechanical response, and resistance to fatigue loadings of microtissue-engineered root dentin. These experiments will provide information on the feasibility of applying root canal dentin microtissue engineering with CSRBnps as a treatment option to enhance the mechanical integrity and, subsequently, the functional requirements in endodontically treated teeth.

MATERIALS AND METHODS

The study protocol and human teeth collection were approved by the university's ethics board (#34853). Teeth were collected and transilluminated before testing to exclude the possibilities of cracks or damages during extraction as well as subjected to radiography to confirm the geometry of the canal system. RB, 1-ethyl-3-(3-dimethylaminopropyl) carbodiimide (EDC), and *N*-hydroxysuccinimide (NHS) were obtained from Sigma-Aldrich (St. Louis, MO). All other chemicals used were of analytical grade (purity ≥95%). Water-soluble carboxymethyl chitosan (CMCS) was synthesized from chitosan powder as described previously[10]. CSRBnps were synthesized by conjugating CSnps with RB[14]. CSnps were synthesized according to the ionic gelation method reported in previous work[15] and chemically cross-linked to RB using EDC (5 mmol/L) and NHS (5 mmol/L). The CSRBnps formed were dialyzed for 1 week; the filtrate was then freeze-dried.

Part 1: Assessment of Dentin Surface Mechanical Properties

Six dentin sections (5 × 5 × 1 mm) with a root canal dentin surface were prepared and polished with SiC abrasive paper (grit size up to 2500) and diamond particle suspensions (size 6 and 0.05 μm) to produce a highly polished surface without imperfections. Specimens were sonicated in 17% EDTA for 3 minutes followed with deionized water at room temperature. Two samples were prepared for each of the following groups:

1. Group CSnps: each dentin specimen was immersed in CSnps in 1% CMCS solution (1 mg/mL) for 30 minutes.
2. Group EDC cross-linked CSnps: each dentin specimen was immersed in CSnps in 1% CMCS solution for 30 minutes followed with 2 mL EDC/NHS (4:1, 33 mmol/L) cross-linker for 8 hours and thereafter washed with deionized water.
3. Group PDA cross-linked CSnps: CSRBnps were dispersed in water and applied on the dentin surface followed by being activated with a noncoherent light for 10 minutes (540 nm, 25 J/cm^2). After washing, each specimen was immersed in CSnps in 1% CMCS solution (1mg/mL) for 15 minutes followed by immersion in RB solution (10 μmol/L) for 15 minutes. The specimens were again exposed to the noncoherent light for 10 minutes and then washed twice.

The dentin specimens were tested under a nanoindenter before and after treatment in each experimental group to serve as its own control and to minimize the variations among individual biological samples.

Nanoindentation was performed using a UNHT^3 NanoIndenter (Anton Paar, Montreal, Quebec, Canada) equipped with a Berkovich diamond indenter with a 100-nm tip radius. Specimens were attached to an 18-mm sample mounting metal disc using cyanoacrylate glue (Krazy Glue original; Elmer's Products, Columbus, OH). The specimen was subjected to quasi-static loading with a maximum load of 1 mN at a loading rate of 3 mN/min and a 30-second holding period at maximum load, which resulted in the penetration of the indenter at around 250–350 nm at the peak load level. During each test, a 6 × 7 grid of a total of 42 indents, spaced apart at approximately 10 μm, were made at the root canal surfaces. Measurements of hardness and elastic modulus from each point were collected and analyzed under the paired sample *t* test to compare the difference between before- and after-treatment dentin samples with a 95% confidence interval (SPSS Statistics Version 20.0; IBM Corp, Armonk, NY).

Part 2: Assessment of Biomechanical Response of Root Dentin

Five of the maxillary incisors were prepared to obtain 12- to 15-mm-long, slab-shaped root specimens with a canal of size F3 (ProTaper Universal F3; Dentsply Sirona, York, PA) following the protocols reported in a previous study[16]. A high-frequency crossline grating (1200 lines/mm), which is the deformation sensing element of a digital moiré interferometry (DMI), was replicated on 1 sagittal side of the tooth section. Samples were subjected to a compressive load from 0–50 N with a 10-N increment under DMI to study the strain distribution of canal preparation under physiological relevant loads. The fringe patterns used for analyzing the strain distribution resulted from the interference between specimen grating and the virtual grating generated from the diode laser (532 nm). Both U (x-axis [perpendicular to dentinal tubules]) and V (y-axis [parallel to dentinal tubules]) directions of the strain distributions were collected. After the first strain investigation conducted with DMI, root canals of the samples were conditioned with PDA cross-linked CSnps. All the specimens were subsequently tested again with DMI. Strain distribution patterns were recorded in each specimen for loads ranging from 0–50 N after root canal instrumentation and microtissue engineering. The strain values were calculated from 6 relative points of interests in both the cervical and apical areas of each sample at each load using image processing software[16]. The collected data were analyzed using a statistical method on trend analysis[16]. The induced strain values from each point were verified by linear regression, and the slope values from the same region/field direction were subjected to a subsequent paired sample *t* test to compare the difference between treatment on dentin with a 95% confidence interval (SPSS Statistics Version 20.0).

TABLE 1 - The Hardness (MPa) and Elastic Modulus (GPa) Resulted before/after Each Treatment Showed Statistical Significance ($P < .01$)

Groups	Hardness (MPa)		Elastic modulus (GPa)	
	Control	After treatment	Control	After treatment
CSnp	284.8 ±115	322.8 ±155	8.14 ± 2.7	7.30 ± 2.5
EDC cross-linked CSnp	395.4 ± 147	276.5 ± 109	9.79 ± 3.5	7.07 ± 2.5
PDA cross-linked CSnp	414.1 ± 119*	431.0 ± 151*	10.27 ± 2.9	12.01 ± 2.9

CSnp, chitosan nanoparticle; EDC, 1-ethyl-3-(3-dimethylaminopropyl)carbodiimide; PDA, photodynamic activated.
*There was no significant difference of hardness in the PDA cross-linked CSnp group ($P > .05$).

Part 3: Assessment of Fatigue Resistance of Root Dentin

Forty-five lower premolar teeth were prepared to obtain 12- to 14-mm-long, slab-shaped root specimens with an F3 canal size (ProTaper Universal F3)[16]. Specimens were subjected to 3 groups: control, EDC cross-linked CSnps, and PDA cross-linked CSnps. In the EDC cross-linked CSnp and PDA cross-linked CSnp groups, the canal space of each dentin specimen was conditioned with nanoparticles followed by chemically or photodynamically cross-linking as described previously.

Root specimens were mounted on brass rings with the roots embedded in self-curing resin (SR-Ivolen Standard Kit; Ivoclar Vivadent, Schaan, Lichtenstein) up to 6 mm apical to the cementoenamel with a 0.2-mm-thick silicone rubber barrier (Aquasil LV; Dentsply DeTrey GmbH, Konstanz, Germany) surrounding the root surfaces to mimic the periodontal ligament. Samples were submitted to stepwise mechanical cycling with a frequency of 15 Hz and a stress ratio of 0.1 with a ball indenter in 100% humidity (Instron, Canton, MA). The stepwise procedure began with a load of 100 N followed by 200, 300, 350, 400, 450, 500, 550, 600, and 650 N at a maximum of 27,000 load cycles each (30 minutes) until failure. Load at failure (N) and the numbers of sustained cycles obtained by the stepwise stress test were recorded and analyzed by Kaplan-Meier and log-rank (Mantel-Cox) tests at a significance of .05 (SPSS Statistics Version 20.0)[17].

RESULTS

Part 1: Assessment of Dentin Surface Mechanical Properties

Table 1 shows the hardness and elastic modulus values obtained from 3 experimental groups with their own control samples. The dentin surface treated with only CSnps showed increased hardness but decreased elastic modulus ($P < .05$). However, the hardness and elastic modulus both reduced significantly after EDC cross-linking CSnps (EDC cross-linked CSnp group) on the dentin surface ($P < .01$), whereas the elastic modulus marginally increased after PDA cross-linking CSnps (PDA cross-linked CSnp group) on the dentin surface ($P < .01$). Figure 1*A–C* shows the biomechanical response of the 3 treatment groups compared with their own control.

Part 2: Assessment of Biomechanical Response of Root Dentin

Strain distribution was analyzed in both the U and V directions. Principally, under the occlusal function, the nature of strain results from the U direction is compressive strain, whereas tensile strain is usually obtained from the V direction. The U field and V field moiré fringe analysis revealed that the compressive loads resulted in a distinct distribution of normal strain along the axial and lateral directions in root dentin. There was a generalized distribution of compressive strain in root dentin, which increased gradually with an increase in the applied loads in both the axial and lateral directions. Figure 2 shows the U field fringe pattern and color map of the root strain distribution patterns before (Fig. 2*A1–4*) and after (Fig. 2*B1–4*) root canal surface microtissue engineering with PDA cross-linked CSnps. After PDA cross-linked CSnp treatment of root canal surface dentin, the U field (*x*-axis) radicular strain at the cervical third and the apical third of root decreased significantly ($P < .01$) (Fig. 3). In the V field (y-axis), root canal surface treated with PDA cross-linked CSnps did not result in a significant difference in strain at the cervical region ($P = .24$) (Fig. 3*A*). However, in the apical third of the root, it resulted in a significant decrease in the magnitude ($P < .01$) and a distinct change in the nature of strain distribution. The postinstrumentation tensile strain at the apical region significantly reduced with the increase of the loads after PDA cross-linked CSnp treatment (Fig. 3*B*).

Part 3: Assessment of Fatigue Resistance of Root Dentin

Survival analysis (Kaplan-Meier and log-rank) of pair-wise comparison showed a statistically significant difference between the control group and the PDA cross-linked CSnp group for load to fracture (log-rank [Mantel-Cox] test, $\chi^2 = 4.78$, $P < .05$) as well as for numbers of sustained cycles until fracture (log-rank test, $\chi^2 = 4.02$, $P < .05$) (Table 2, Fig. 4*A* and *B*). The PDA cross-linked CSnp group exhibited the highest fatigue failure loads and numbers of

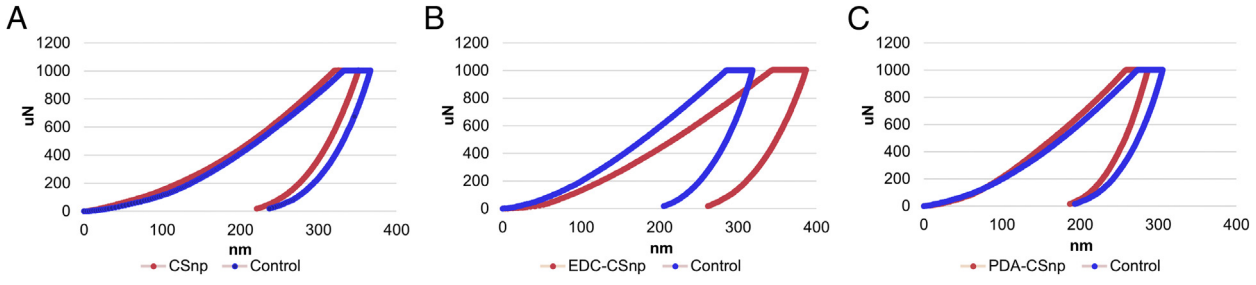

FIGURE 1 – The load-displacement curves resulted from each group by nanoindentation. The surface treated with (*A*) CSnps and (*C*) PDA cross-linked CSnps showed stiffer behavior compared with the control. (*B*) It resulted in softer behavior in specimens treated with EDC cross-linked CSnps.

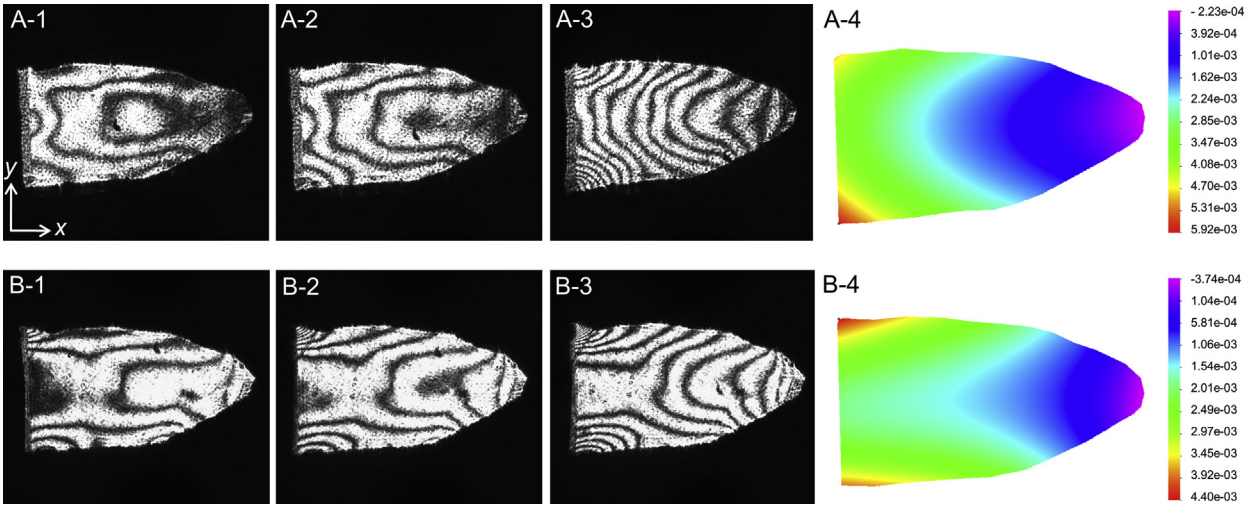

FIGURE 2 – (*A-1–3*) Fringe patterns in the U field at 10-, 20-, and 40-N loads in root dentin before microtissue engineering with PDA cross-linked CSnps. (*A-4*) A color map obtained the fringe analysis showing the whole-field displacement of sample before microtissue engineering with PDA cross-linked CSnps. (*B-1–3*) Fringe patterns in the U field at 10-, 20-, and 40-N loads shown in microtissue-engineered root dentin. (*B-4*) A color map obtained the fringe analysis showing the whole-field displacement of the sample after engineering the root dentin with CSnps.

sustained cycles to failure, whereas the control group exhibited the lowest values (Table 2).

DISCUSSION

Nanoindentation is effective in determining the elastic modulus and hardness of a microstructure[18]. This approach was used in the current study to evaluate the surface mechanical properties of root canal dentin cross-linked with nanoparticles. The elastic modulus of intertubular dentin is around 16–21 GPa, which may decrease to 3–19 GPa in proximity to pulp[19]. In the current study, the averaged elastic modulus of root canal dentin determined before microtissue engineering was 8–10 GPa, which was comparable with previous studies[19,20]. The mean hardness values ranged from 300–400 MPa, which was marginally higher than the data obtained from Kinney et al[18]. This difference may be attributed to the difference in the experimental parameters set during measurement[18]. Dentin cross-linking is used to improve the mechanical characteristics and stability of hard tissue by inducing covalent bonds between collagen molecules. Previous studies showed higher stiffness, elastic modulus, and mechanical properties of nondemineralized/demineralized dentin with chemical or PDA

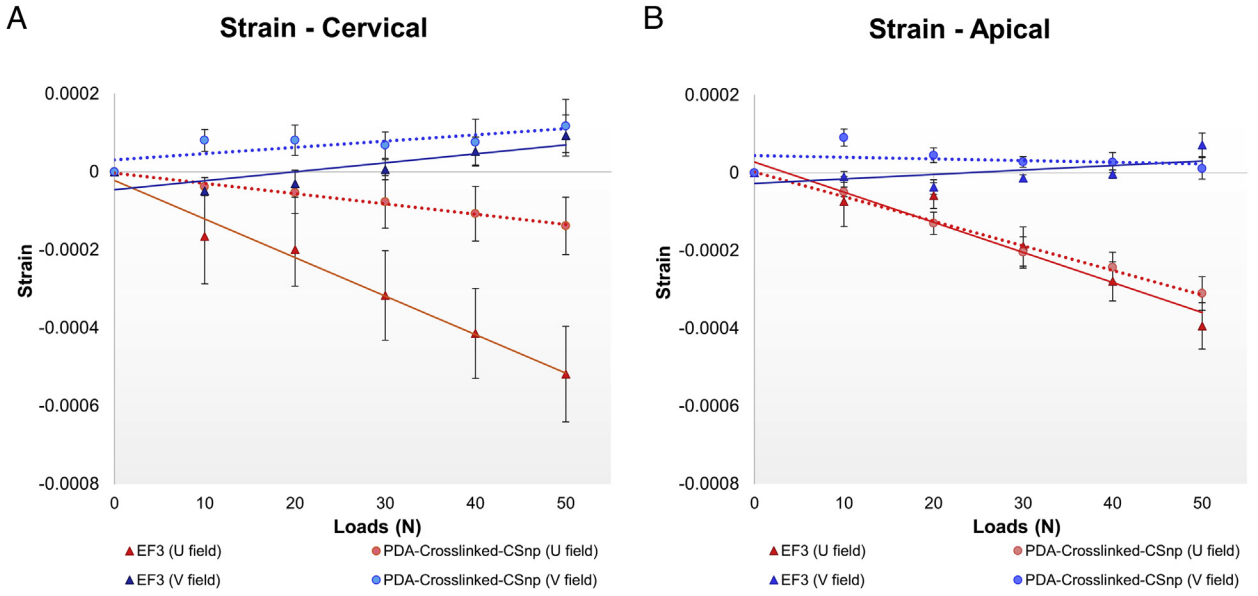

FIGURE 3 – Strain values in the U and V fields generated from the (*A*) cervical and (*B*) apical third of the root before and after microtissue engineering with PDA cross-linked CSnps on the root dentin surface. The root strain formed after the root canal surface was engineered with PDA cross-linked CSnps was significantly less compared with the root strain obtained after instrumentation for loads ranging from 10–50 N in the U field ($P < .01$). Moreover, the apical tensile strain in the V field resulted in a decreased trend with the increase of loads on microtissue-engineered root dentin ($P < .01$).

TABLE 2 - Experimental Design and Mean (± Standard Deviation) of the Sustained Load (N) and Numbers of Cycles at Failure

Groups	Experimental procedures	Load at failure (N)	Sustained cycles at failure (*n*)
Control	Root canal prepared	412.5 ± 80.1	137,223.1 ± 43,534.8
EDC cross-linked CSnp	Root canal prepared + CSnp + EDC cross-link	477.3 ± 81.7	159,716.5 ± 51,473.4
PDA cross-linked CSnp	Root canal prepared + CSnp + PDA cross-link	489.3 ± 68.4	174,397.7 ±37,143.5

CSnp, chitosan nanoparticle; EDC, 1-ethyl-3-(3-dimethylaminopropyl)carbodiimide; PDA, photodynamic activated.

cross-linking[14,21,22]. The reduced hardness and elastic modulus of the EDC cross-linked CSnp dentin surface resulted mainly from EDC cross-linking. It was not consistent with earlier reports of 1.5–3 times higher stiffness in EDC cross-linked demineralized dentin[22]. Nevertheless, softer surface properties of EDC cross-linked scaffolds compared with glutaraldehyde cross-linked scaffolds have been reported[11]. Further investigation is required to explain this mechanism. Conversely, dentin surface treated with PDA cross-linked CSnps resulted in higher mean elastic modulus.

DMI is an established highly sensitive, optical interferometry–based technique to evaluate the biomechanical response of dento-osseous structures under physiologically relevant loads[16,23,24]. In the present study, both cervical and apical root dentin were analyzed because functional stress/strain is predominantly distributed at the cervical root dentin, whereas increased root flexure and apical stress/strain have been reported in root-filled teeth[5,25,26]. Previous investigations showed that instrumented root canal dentin exhibited reduced stability with increased deformation and radicular tensile strain[16]. This alteration in the biomechanical response of root dentin may increase the risk of structural failure with time. The findings from the current study showed decreased strain distribution in the microtissue-engineered dentin when compared with instrumented root dentin. In addition, microtissue engineering of root canal dentin also resulted in the reduction of apical tensile strain while uniformly distributing compressive strain in the direction perpendicular to the dentinal tubules (U field). The reduction in apical tensile strain and decreased strain distribution contribute to diminished root flexure and enhanced mechanical stability in root-filled teeth[27,28].

VRF in root-filled teeth is considered to be a fatigue process, mainly because of cyclic load–induced subcritical crack growth in response to chewing[29]. Fatigue loads generated cyclic stress/strain in a structure and contributed to crack initiation, crack propagation, and catastrophic failure with time. The cracks formed would behave as stress concentrators to initiate crack propagation when the stress magnitude is high enough to induce microscopic plastic deformation at the crack tip[5]. Fatigue strength is an important parameter for assessing the ability of a root to resist fracture while in function. Mechanical cycling, which simulates mastication cycles in the mouth, can be simulated in the laboratory by an intermittent loading setup with controlled parameters such as load, numbers of cycles, and frequency[30]. Earlier investigations have proposed 1 million cycles of loading to simulate 1–5 years of chewing function[29,31]. According to the preliminary test, subjecting the specimen to a clinical level of loads (50–150 N) for 1 million cycles was not able to induce consistent crack propagation and subsequent catastrophic fracture of teeth. Therefore, the stepwise loading methodology, which started from 100 N with 50/100-N increments every 27,000 cycles, was found to be more appropriate for this investigation[17,32]. Evaluation of the strain distribution pattern physiologically relevant loads using DMI and fatigue resistance using cyclic loading provided a better insight regarding the mechanical characteristics of the root dentin after instrumentation and microtissue engineered with cross-linked CSnps[33].

In the current study, the enhanced mechanical properties including reduced radicular strain, apical tensile strain, and increased fatigue resistance in microtissue-

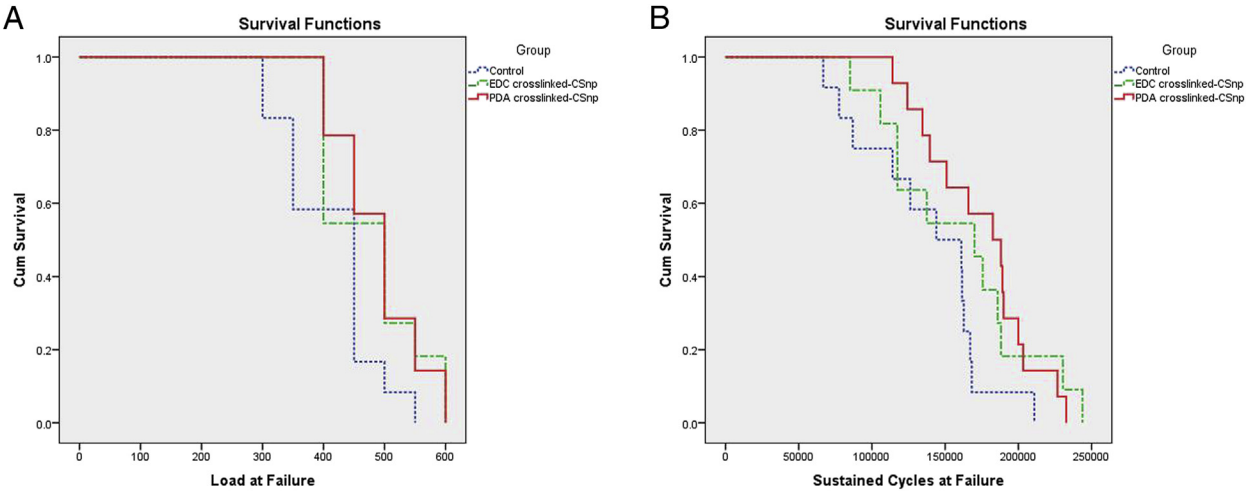

FIGURE 4 – Survival curves according to the (*A*) steps of loads and (*B*) numbers of cycles for each failed tooth. (control group: *blue*; EDC cross-linked CSnp group: *green*; PDA cross-linked CSnp group: *red*).

engineered root dentin can be explained by the following mechanisms. In microtissue engineering, CSnps interacted well and formed a conditioning layer on the root canal dentin[8,15]. Negatively charged dentin collagen and positively charged CSnps form polyanion-polycation ionic complexes[15,34]. The coated CSnps would also impart additional antibacterial properties on root canal dentin. The integration of CSnp/CMCS in between collagen molecules and collagen fibrils served as hydrophilic spacers to facilitate water holding characteristics, flexibility, and load transfer/energy absorption characteristics during mechanical functions[9,10]. In addition to coating, cross-linking the CSnps to dentin tissue may further amplify the strengthening effect brought about by CSnps on dentin matrix. The process of cross-linking introduces covalent bonds between CSnp-collagen and collagen-collagen, which will aid in retaining the resistance to bacterial-mediated enzymatic degradation in root canal dentin[14].

During photodynamic cross-linking, the singlet oxygen or radical is produced by a light-activated photosensitizer. The highly active singlet oxygen produced by the light-activated photosensitizer induces photo-oxidation of photo-oxidizable amino acid residues, which further react with normal or photo-altered residues in another protein molecule to induce a cross-link[35]. RB is 1 of the photosensitizers that can be activated with green light (λ = 520–560 nm) to form photodynamic cross-linking. Photodynamic cross-linking is considered a rapid, efficient method with low cytotoxicity to induce covalent bonds for stabilizing the collagen-based biomaterials and can be incorporated practically into clinical procedures. Along similar lines, earlier experiments that cross-linked dentin collagen with chitosan derivatives exhibited improved toughness[10,14].

The current study indicates that microtissue-engineered root canal dentin enhanced the mechanical characteristics of the root dentin. Cross-linking the instrumented root canal with CSnps photodynamically improved the biomechanical response of the root, resulting in a significantly decreased compressive strain at the cervical region in the direction perpendicular to the dentinal tubules and a reduction in the apical tensile strain in the direction parallel to the dentinal tubules. Also, microtissue engineering of root canal dentin resulted in roots with higher fatigue load/sustained cycles to failure. These changes in the biomechanical response of root dentin have the potential to improve the resistance to root fracture in endodontically treated teeth.

ACKNOWLEDGMENTS

Supported in part by a research grant from the American Association of Endodontists Foundation (grant no. 505328), the University of Toronto (grant no. 206760) (A.K.), Natural Sciences and Engineering Research Council of Canada (grant no. 04642), and the Canadian Foundation for Innovation (grant no. 493891) (A.K.).

The authors deny any conflicts of interest related to this study.

REFERENCES

1. Touré B, Faye B, Kane AW, et al. Analysis of reasons for extraction of endodontically treated teeth: a prospective study. J Endod 2011;37:1512–5.
2. Olcay K, Ataoglu H, Belli S. Evaluation of related factors in the failure of endodontically treated teeth: a cross-sectional study. J Endod 2018;44:38–45.
3. Kishen A. Mechanisms and risk factors for fracture predilection in endodontically treated teeth. Endod Topics 2006;13:57–83.
4. Tang W, Wu Y, Smales RJ. Identifying and reducing risks for potential fractures in endodontically treated teeth. J Endod 2010;36:609–17.
5. Kishen A. Biomechanics of fractures in endodontically treated teeth. Endod Topics 2015;33:3–13.
6. Rashidi H, Yang J, Shakesheff KM. Surface engineering of synthetic polymer materials for tissue engineering and regenerative medicine applications. Biomater Sci 2014;2:1318–31.
7. Sung HW, Chang Y, Chiu CT, et al. Crosslinking characteristics and mechanical properties of a bovine pericardium fixed with a naturally occurring crosslinking agent. J Biomed Mater Res 1999;47:116–26.
8. Kishen A, Shrestha S, Shrestha A, et al. Characterizing the collagen stabilizing effect of crosslinked chitosan nanoparticles against collagenase degradation. Dent Mater 2016;32:968–77.
9. Madhavan K, Belchenko D, Motta A, Tan W. Evaluation of composition and crosslinking effects on collagen-based composite constructs. Acta Biomater 2010;6:1413–22.
10. Shrestha A, Friedman S, Kishen A. Photodynamically crosslinked and chitosan-incorporated dentin collagen. J Dent Res 2011;90:1346–51.
11. Oryan A, Kamali A, Moshiri A, et al. Chemical crosslinking of biopolymeric scaffolds: current knowledge and future directions of crosslinked engineered bone scaffolds. Int J Biol Macromol 2018;107:678–88.
12. Chan BP, Hui TY, Chan OC, et al. Photochemical cross-linking for collagen-based scaffolds: a study on optical properties, mechanical properties, stability, and hematocompatibility. Tissue Eng 2007;13:73–85.

13. Wollensak G, Iomdina E. Long-term biomechanical properties of rabbit sclera after collagen crosslinking using riboflavin and ultraviolet A (UVA). Acta Ophthalmol 2009;87:193–8.

14. Shrestha A, Hamblin MR, Kishen A. Photoactivated rose bengal functionalized chitosan nanoparticles produce antibacterial/biofilm activity and stabilize dentin-collagen. Nanomedicine 2014;10:491–501.

15. Kishen A, Shi Z, Shrestha A, Neoh KG. An investigation on the antibacterial and antibiofilm efficacy of cationic nanoparticulates for root canal disinfection. J Endod 2008;34:1515–20.

16. Li FC, Kishen A. Microtissue engineering root canal dentine with crosslinked biopolymeric nanoparticles for mechanical stabilization. Int Endod J 2018;51:1171–80.

17. Missau T, De Carlo Bello M, Michelon C, et al. Influence of endodontic treatment and retreatment on the fatigue failure load, numbers of cycles for failure, and survival rates of human canine teeth. J Endod 2017;43:2081–7.

18. Kinney JH, Balooch M, Marshall SJ, et al. Hardness and Young's modulus of human peritubular and intertubular dentine. Arch Oral Biol 1996;41:9–13.

19. Ryou H, Amin N, Ross A, et al. Contributions of microstructure and chemical composition to the mechanical properties of dentin. J Mater Sci Mater Med 2011;22:1127–35.

20. Kishen A, Ramamurty U, Asundi A. Experimental studies on the nature of property gradients in the human dentine. J Biomed Mater Res 2000;51:650–9.

21. Liu X, Zhou J, Chen L, et al. UVA-activated riboflavin improves the strength of human dentin. J Oral Sci 2015;57:229–34.

22. Ryou H, Turco G, Breschi L, et al. On the stiffness of demineralized dentin matrices. Dent Mater 2016;32:161–70.

23. Kishen A, Asundi A. Experimental investigation on the role of water in the mechanical behavior of structural dentine. J Biomed Mater Res A 2005;73:192–200.

24. Li F, Kishen A. Deciphering dentin tissue biomechanics using digital moire interferometry: a narrative review. Opt Laser Eng 2018;107:273–80.

25. Kishen A, Asundi A. Photomechanical investigations on the stress-strain relationship in dentine macrostructure. J Biomed Opt 2005;10:034010.

26. Rivera EM, Walton RE. Longitudinal tooth cracks and fractures: an update and review. Endod Topics 2015;33:14–42.

27. Nalla RK, Kinney JH, Ritchie RO. On the fracture of human dentin: is it stress- or strain-controlled? J Biomed Mater Res A 2003;67:484–95.

28. Lang H, Korkmaz Y, Schneider K, Raab WH. Impact of endodontic treatments on the rigidity of the root. J Dent Res 2006;85:364–8.

29. Nalla RK, Imbeni V, Kinney JH, et al. *In vitro* fatigue behavior of human dentin with implications for life prediction. J Biomed Mater Res A 2003;66:10–20.

30. Mair L, Padipatvuthikul P. Variables related to materials and preparing for bond strength testing irrespective of the test protocol. Dent Mater 2010;26:e17–23.

31. Wiskott HW, Nicholls JI, Belser UC. Stress fatigue: basic principles and prosthodontic implications. Int J Prosthodont 1995;8:105–16.

32. Fennis WM, Kuijs RH, Kreulen CM, et al. Fatigue resistance of teeth restored with cuspal-coverage composite restorations. Int J Prosthodont 2004;17:313–7.

33. Tan PL, Aquilino SA, Gratton DG, et al. *In vitro* fracture resistance of endodontically treated central incisors with varying ferrule heights and configurations. J Prosthet Dent 2005;93:331–6.

34. Taravel MN, Domard A. Relation between the physicochemical characteristics of collagen and its interactions with chitosan: I. Biomaterials 1993;14:930–8.

35. Spikes JD, Shen HR, Kopecková P, Kopecek J. Photodynamic crosslinking of proteins. III. Kinetics of the FMN- and rose bengal-sensitized photooxidation and intermolecular crosslinking of model tyrosine-containing N-(2-hydroxypropyl)methacrylamide copolymers. Photochem Photobiol 1999;70:130–7.